Inflammopharmacology (2020) 28:1525–1536
https://doi.org/10.1007/s10787-020-00723-5

Inflammopharmacology

ORIGINAL ARTICLE

The protective effect of *Sophora japonica* on prostatic hypertrophy and inflammation in rat

Ahmed Elberry[1] · Shagufta Mufti[2] · Jaudah Al-Maghrabi[3] · Salah Ghareib[4] · Hisham Mosli[5] · Ali El-Halawany[6] · Essam Abdel-Sattar[6]

Received: 20 April 2020 / Accepted: 11 May 2020 / Published online: 5 June 2020

Abstract

The atypical adenomatous hyperplasia (AAH) is invariably an incidental histological change, with no clinical findings specific for its diagnosis, and the mean patient age at diagnosis is 64–70 years. The incidence of AAH varies between 1.5 and 19.6% of transurethral resections and in up to 33% of radical prostatectomies. Herbal medicines are becoming a popular option in the treatment of prostatic-related diseases, such as date palm pollen and saw palmetto in the treatment of prostatic hyperplasia. A testosterone/citral-induced AAH in Wistar rat model was used to evaluate the protective effect of *Sophora japonica* fruit extract (SFE). The present study suggests that SFE has an ameliorating effect on the prostatic hypertrophy and inflammation through its effect on clusterin, IGF, IL-6, IL-8, TNF-α, and TGF-β1 expression. In addition, the administration of SFE ameliorated the inflammatory score, and histopathological changes in AAH-induced rats in a dose-dependent manner. The treatment with SFE reduced the number of prostatic acini in AAH rat model and decreased the production of pro-inflammatory cytokines. The fruit extract of *S. japonica* was characterized by determination total phenol content (60.3 mg of gallic acid equivalent/g of dry extract), total flavonoid content (97.9 mg quercetin equivalent/g of dry extract) and the major isoflavonoid sophoricoside (302.9 ± 2.6 µg/g of the extract). In conclusion, SFE has an ameliorating effect on the prostatic hypertrophy and inflammation. This effect may be attributed to the ability of SFE to decrease the production of pro-inflammatory cytokines, TNF-α, IL-1β and IGF-1 as well as an increase in TGF-β1.

Keywords *Sophora japonica* · Atypical adenomatous hyperplasia · Prostatic hypertrophy · Pro-inflammatory cytokines · TGF-β1 expression

Introduction

Atypical adenomatous hyperplasia (AAH) is a pseudoneoplastic lesion that can be confused with prostate adenocarcinoma (PAC) and characterized by the proliferation of small glands in the prostate with imbalance between prostate cell growth and apoptosis (Montironi et al. 2007; Sciarra et al. 2008). It is considered as an intermediate lesion between benign prostate hyperplasia (BPH) and PAC (Bostwick et al. 1993). The AAH is invariably an incidental histological finding, and there are no clinical findings specific for it and the mean patient age at diagnosis is 64–70 years (Humphrey 2012). The incidence of AAH varies between 1.5 and 19.6% of transurethral resections and in up to 33% of radical

Electronic supplementary material The online version of this article (https://doi.org/10.1007/s10787-020-00723-5) contains supplementary material, which is available to authorized users.

✉ Ahmed Elberry
berry_ahmed@yahoo.com

✉ Essam Abdel-Sattar
essam.abdelsattar@pharma.cu.edu.eg

[1] Department of Pharmacology, Faculty of Medicine, Beni-Suef University, Beni Suef 62511, Egypt

[2] Department of Pathology, Era's Medical College, Era University, Lucknow, UP, India

[3] Department of Pathology, Faculty of Medicine, King Abdulaziz University, Jeddah, Saudi Arabia

[4] Department of Pharmacology, Faculty of Pharmacy, Zagazig University, Zagazig, Egypt

[5] Department of Urology, Faculty of Medicine, King Abdulaziz University, Jeddah, Saudi Arabia

[6] Department of Pharmacognosy, Faculty of Pharmacy, Cairo University, Kasr El-Aini Street, Cairo 11562, Egypt

prostatectomies (Enciu et al. 2012). It was suggested that immunoinflammatory stimulators might play a role in the prostatic epithelial cell growth by modulating the cytokine system and might promote hyperplastic changes (Gleason et al. 1993; KESSLER et al. 1998). Chronic Inflammation produces free radicals as various reactive oxygen species (Rigas and Sun 2008).

Because of many side effects of drug therapy and surgical procedures, herbal medicines are becoming a popular option in the treatment of prostatic disease. *Sophora japonica* L. (SF) is a traditional Chinese medicine known as Kushen and it has been commonly used for the treatment of viral hepatitis, cancer, viral myocarditis, gastrointestinal hemorrhage, and skin diseases such as eczema and psoriasis (Chinese-Pharmacopoeia-Commission 2010). Quinolizidine alkaloids and flavonoids are the major active constituents of this plant. Alkaloids exhibit many pharmacological effects including sedative, analgesic, antipyretic, and anti-arrhythmic actions (Zhang et al. 2015). Matrine and oxymatrine are the main alkaloids of SF and was reported to have anticancer and anti-inflammatory effect (Ho et al. 2009; Zhang et al. 2011). On the other hand, flavonoids have been also known for their antioxidant, anti-proliferative and anti-inflammatory activities (Jin et al. 2010; Zhou et al. 2009). Moreover, Kushen flavonoids have been found to exert more potent antitumor activities than Kushen alkaloids and has also antiangiogenic activity (Pu et al. 2013; Sun et al. 2012). The aim of the current study was to investigate the possible protective effect of the SF methanolic extract on enlarged rat prostate and the histopathological changes related to inflammation, proliferation and/or apoptosis in AAH-induced experimentally in rats.

Materials and methods

Chemicals and reagents

Solvents of HPLC grade were used for HPLC analysis, in addition to analytical grade solvents for extraction and thin-layer chromatography (TLC) which were purchased from Sigma-Aldrich (St. Louis, MO, USA). Antibodies against clusterin, phospho-Smad2, and β-actin were obtained from Santa Cruz Biotechnology (Santa Cruz, CA; anti-clusterin for Western blot analysis); Upstate Biotechnology [Lake Placid, NY; anti-clusterin for immunohistochemistry (IHC)]; and Cell Signaling Technology Inc. (Danvers, MA). Antibody against TGF-β1 ligands were purchased from Dakocytomation (Carpinteria, CA). Citral was obtained from Fluka Chemie AG, Buchs, Switzerland. Testosterone was obtained from Sigma-Aldrich and Dakocytomation (Carpinteria, CA); while, saw palmetto was obtained from Futurebiotics (NY, USA).

Plant materials and extraction

The fruits of *S. japonica* were collected from the Experimental Station of Faculty of Pharmacy, Cairo University, in April 2010. The plant was identified by the staff of the Department of Biology, Faculty of Science, King Abdulaziz University. A sample was kept at the Herbarium of the Department of Natural Products and Alternative Medicine, Faculty of Pharmacy, King Abdulaziz University. The plant materials were air dried and subjected to grinding; then kept in dark air-tight closed containers until the extraction step.

Powdered fruits of *S. japonica* (300 g) were extracted with methanol (3 × 2000 mL) using Ultra-Turrax T25 homogenizer. The solvents were distilled off under reduced pressure to give 152 g of yellowish-brown extract, which then lyophilized and kept at 4 °C till biological tests.

Characterization of *S. japonica* extract

Determination of total phenol and flavonoid content

The phenolic content of *S. japonica* L. extract was measured using the Folin–Ciocalteu method (Singleton and Rossi 1965) with the modifications proposed by (Abdel-Sattar et al. 2014). The total phenolic content was determined by measuring the absorbance at 685 nm using gallic acid as a reference standard (0.02–0.30 mg/mL) and the result was expressed in milligram equivalents of gallic acid per gram of dry extract. In addition, the total flavonoid content in the extract was determined using a previously described aluminum chloride colorimetric assay, which relies on quantifying the formation of flavonoid–aluminum complexes by measuring the absorbance at 430 nm (Lamaison et al. 1990). Quercetin was used as a reference standard (0.03–0.30 mg/mL). The total flavonoid content was expressed in milligram equivalents of quercetin per gram of dry extract.

High-performance liquid chromatography (HPLC) analysis

Dried fruit powder (500 mg) was extracted with methanol (2 × 10 mL, HPLC grade) using ultra sonic bath for 15 min, and then the volume was made 25 mL with methanol. HPLC analysis was performed on Agilent HP1200 series HPLC system equipped with a G1322A quaternary pump and degasser, a photodiode array detector (PDA). The flow rate was maintained at 1.0 mL/min and UV monitored at 320, 280 and 254 nm. Chromatographic separations were performed on an Agilent ZORBAX Eclipse XDB-C18 (150 × 4.6 mm i.d., 5 µm), including C-18 guard column. Prior to HPLC analysis, all samples were filtered using Millex-HV filters (Millipore, Bedford, MA, USA) with

0.45-mm pore size. Injection volume was 20 µL. Sophoricoside was selected for standardization process as an external standard (Abdallah et al. 2014). A standard calibration curve was established in the detector linear range from 25 to 1000 µg/mL (supplementary data). For gradient elution, mobile phases A and B were employed. A; 0.1% TFA in water and B was acetonitrile. The following linear gradient was used: from 0% B/A to 20% B/A in 10 min, then to 50% B at 15 min, from 50% to 100% B at 20 min and 100% B till 22 min then returning back to 100% A at 25 min. Under the previous conditions, sophoricoside was eluted at 13.98 min.

Biological assay

Animals Adolescent male Wistar rats, aged 50–60 days, were obtained from the animal facility of King Fahd Research Center, King Abdulaziz University, Jeddah, Saudi Arabia. They were used in the study according to the guidelines of the Biochemical and Research Ethics Committee at King Abdulaziz University, following the NIH guidelines. Animals were housed in a well-ventilated, temperature-controlled room at 22 ± 3 °C with a 12-h light–dark cycle. They were provided with standard rat chow pellets obtained from Grain Silos and Flour Mills Organization F-1005, Jeddah, Saudi Arabia and tap water ad libitum. All experimental procedures were performed between 8 and10 a.m. and care was taken to avoid stressful conditions.

Experimental design Orchidectomy was performed aseptically, under ketamine anesthesia, by a midscrotal incision. Following ligation of the spermatic cord and vessels, testes and epididymis were removed. The remaining stump was pushed back through the inguinal canal into the abdominal cavity, and the scrotal sac was closed by sutures (Golomb et al. 1998). After castration, the rats were maintained under standard laboratory conditions for 7 days to allow a definite involution of the prostatic gland (Sandford et al. 1984).

The AAH was induced as previously described by (Engelstein et al. 1996). In castrated rats using citral and testosterone, rats were subcutaneously injected with testosterone propionate in corn oil (0.5 mg/0.1 mL/rat) each day for 30 days. Citral, 1 M diluted in 70% ethanol, was smeared on a different shaved area of skin, each time, on the back at a final dose of 185 mg/kg every 4 days for 30 days. Control group rats were smeared with the solvent (ethanol) alone at the shaved skin. Considering the pungent lime fragrance of citral, the control groups were kept in a separate location from the citral-treated animals to avoid possible false results as citral have some influence via the olfactory tract.

Animal treatment Seven days after castration, the animals were randomly divided into six groups ($n = 7$). Group I served as control (shamed operation) received corn oil (0.1 mL/rat) and 1% CMC-Na (0.3 mL/100 g body weight) daily during the period of the experiment. Groups from II to VI were castrated and had AAH. Group II served as negative control and received CMC-Na 1% as previously mentioned. Group III served as positive control and received Saw Palmetto (100 mg/kg) suspended in 1% CMC-Na. Groups from IV to VI were treated with SFE at doses of 75, 150 or 300 mg/kg/day, respectively, by oral gavage. All the SFE were suspended in 1% CMC-Na and were given to rats once daily by oral gavage along with testosterone injection and citral smearing for 30 days as described before (SCOLNIK et al. 1994). After euthanization, ventral prostate of each rat in each group was removed from the body, 24 h after the last administration, and weighed. The prostate index (PI) was calculated as 'prostate weight/rat body weight × 100'. The half of the tissues were frozen in liquid nitrogen and stored at -75 °C until use. The remaining tissues were fixed immediately in 0.1-M phosphate-buffered 10% formalin (pH 7.4) for 48 h and then embedded in paraffin and were used for histological studies. Serial 4-µm-thick sections from each tissue specimen were prepared and mounted on poly-L-lysine-coated glass slides. These were used for detection of IL-6, IL-8, TNF-α, IGF-1, clusterin and TGF-β1 receptors in the prostatic tissue by immunohistochemistry.

Histopathology and histoscore A part of the ventral lobes was separated and fixed overnight in Stieve's solution. Thereafter, the tissue was thoroughly rinsed with water, and immersed overnight in ethanol 70%. Then, it was dehydrated, embedded in paraffin, and 5-mm-thick sections were cut and stained by Harris' hematoxylin–eosin, according to the standard procedures of (Lillie and Fullmer 1965).

A score-chart protocol (histoscore) developed by (SCOLNIK et al. 1994) was used to obtain an objective quantitative assessment. The examination, description, and scoring of the slides were performed in a blinded manner. The scoring system presented in arbitrary units to make a better evaluation. In a second step, the cumulative score in each group was correlated with the final histological diagnosis to establish a range score for normal and hyperplasia. Additional histological inflammatory score described by (De Nunzio et al. 2011) was used to evaluate the inflammation. Score 0: no inflammation, score 1: scattered inflammatory cell infiltrate without nodules, score 2: no confluent lymphoid, and score 3: large inflammatory areas with confluence.

Immunohistochemistry and immunohistoscoring Staining with hematoxylin and eosin was performed to observe the histopathological changes. For analysis of IL-6 and TGF-β1 expression, sections from the paraffin-embedded tissue blocks were mounted on charged glass slides and baked at 60 °C for 1 h in the oven, then mounted on the Ventana staining machine, dewaxed by EZ Prep (xylene substitute)

and rehydrated. The tissue sections were heated in Ventana buffer CC1 (pH 6) to facilitate antigen retrieval, then treated with H_2O_2 to eliminate endogenous peroxidase. This was followed by incubation for 60 min at room temperature with primary antibodies IL-6 and TGF-β1. The dilutions used were; IL-6 (dilution 1:50) and TGF-β1 (dilution of 1:25). Subsequently, the sections were incubated with biotinylated secondary antibody using avidin–biotin complex method. The immunoreaction was visualized using diaminobenzidine. All the sections were lightly counterstained with hematoxylin as a background. The positive control used for IL-6 and TGF-β1 was from the colon. The negative controls comprised serial sections that were stained using equivalent concentrations of nonimmune mouse IgG in place of the primary antibodies. The level of staining was evaluated independently by three observers blinded to experimental conditions.

Expression of TGF-β1 and IL-6 was evaluated according to a semiquantitative scale: score 0, no detectable staining at all; score 1, less than 10% of the cells stained positive; score 2, 10–50% positive cells; and score 3, more than 50% of cells positive (Hobisch et al. 2000). Staining intensity was scored as score 0, score 1 (weak staining detected at intermediate to high power), score 2 (moderate detected at low to intermediate power) to score 3 (strong detected at low power) (Gounder et al. 2008).

Reverse transcription polymerase chain reaction (RT-PCR) Total RNA was extracted from the snap-frozen tissue samples using total RNA isolation kit (Macherey–Nagel) according to the manufacturer's instructions. RT was performed in a 10-µL reaction mixture. The RT reaction contained 1-µg RNA, 10-mM Tris–HCl (pH 8.3), 50-mM KCl, 1.5-mM MgCl2, 2.5-mM dithiothreitol, 500 µmol/L each of dATP, dCTP, dGTP, and dTTP (Bioline), 40-U RNasin (Bioline), 25-µg/mL oligo dT_pd (T)12–18 (Bioline) and 100-U Moloney murine leukemia virus reverse transcriptase (Bioline). The reaction mixture was incubated at 42° C for 60 min and then heated to 80° C for 5 min. The resultant cDNA was used for PCR. For quantitative real-time RT-PCR, we prepared appropriate dilutions of each single-strand cDNA followed by normalizing of the cDNA content using β-actin as a quantitative control. Quantitative PCR amplification was performed with a 25-µL final volume consisting of 1-µL RT reaction mixture, 3-mM $MgCl_2$, 10 pmol of each sense and antisense primer, and 12.5 µL (Roche Diagnostics). PCR conditions were as follows: initial denaturation at 95 °C for 10 min and 35 cycles of denaturation at 94 °C for 1 min, annealing at 55 °C for 1 min, and elongation at 72 °C for 2 s with a final elongation at 72 °C for 10 min. Samples were migrated in 1% agarose gel using electrophoresis, UV visualized, and images were analyzed using total lab120 (Nonlinear Dynamic Ltd). Clusterin, TGF-β1, IGF-1, IL-6, IL-8, and TNF-α expression in the test samples were normalized to the corresponding β-actin level and were reported as the relative band intensity to the β-actin gene expression. Sequences of oligonucleotides used as primers for β-actin, IL-6, IL-8, TNFα, TGF-β1, IGF-1 and clusterin are summarized in Table 1.

Statistical analysis

Data were expressed as mean ± SE and were analyzed by analysis of variance (ANOVA) followed by Tukey–Kramer multiple comparisons test. Inflammation scores and their significance were calculated by Chi square test with Yate's corrections. Differences were considered significant with a *P* value less than 0.05. Statistical analyses were performed using the SPSS for Windows (v. 10.0).

Results

Characterization of *S. japonica* fruit extract

Assay of total phenol content of the methanolic extract of *S. japonica* fruit was determined to be 60.3 mg of gallic acid equivalent/g of dry extract. Assay of total flavonoid content was determined to be 97.9-mg quercetin equivalent/g of dry extract. HPLC analysis (Figs. 1 and 2) revealed the presence of sophoricoside as the main isoflavonoid phenolic glycoside *of S. japonica* fruit at concentration of 302.9 ± 2.6 µg/g of extract.

Table 1 Sequences of oligonucleotides used as primers

Gene	Forward primer	Reverse primer
β-Actin	5′-GTCACCCACACTGTGCCCATCT-3	5′-ACAGAGTACTTGCGCTCAGGAG-3′
IL-6	5′-GAACTCCTTCTCCACAAGCG-3′	5′-TTTTCTGCCAGTGCCTCTTT-3′
IL-8	5′-CTGCGCCAACACAGAAATTA-3′	5′-ATTGCATCTGGCAACCCTAC-3′
TNF-*α*	5′-CAGAGGGAAGAGTTCCCCAG-3′	5′-CCTTGGTCTGGTAGGAGACG-3′
TGF-*β*1	5′-GTTCTTCAATACGTCAGACATTCG-3′	5′-CATTATCTTTGCTGTCACAAGAGC-3′
IGF-1	5′-CACAGGCTATGGCTCCAGCAT-3′	5′-TCTCCAGCCTCCTCAGATCACA-3′
Clusterin	5′-CTGACCCAGCAGTACAACGA-3′	5′-TGACACGAGAGGGGACTTCT-3′

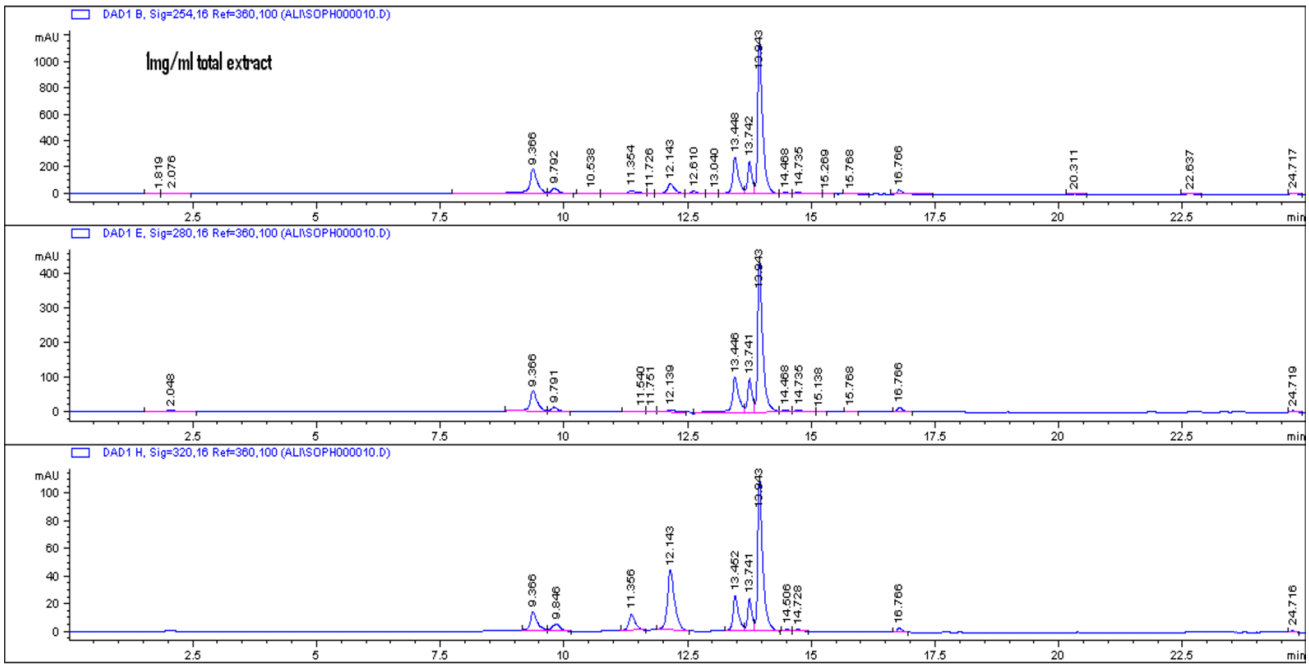

Fig. 1 HPLC chromatogram of total alcoholic extract of *Sophora* fruit extract at 254, 280 and 320 nm

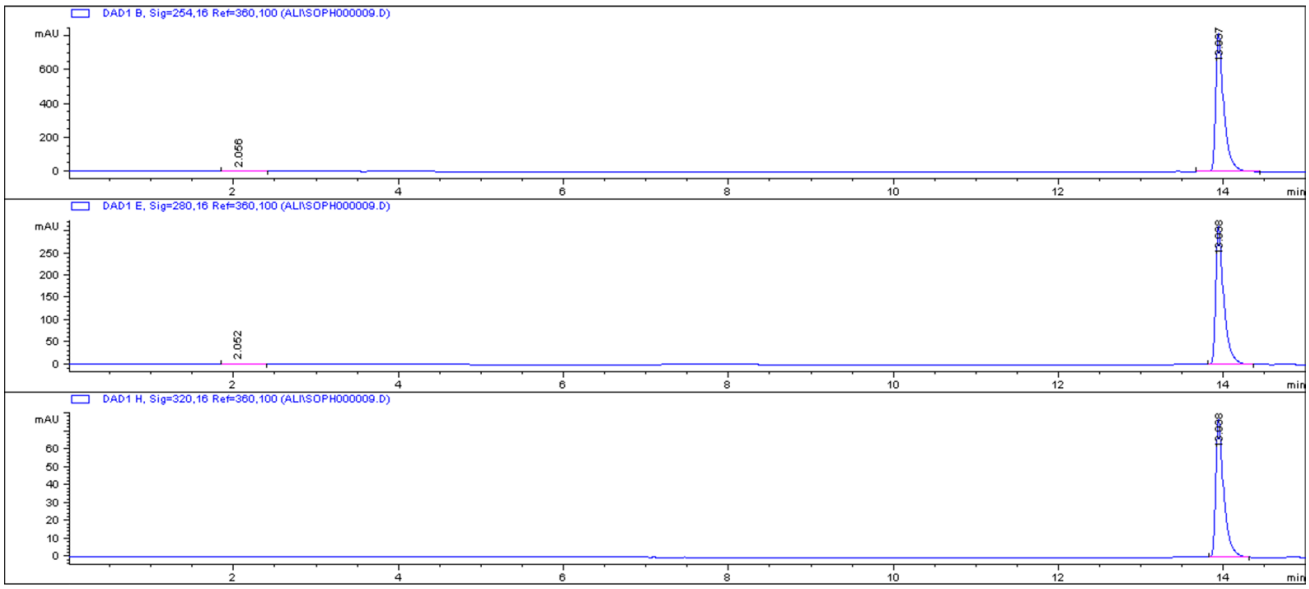

Fig. 2 HPLC chromatogram of sophoricoside at 254, 280 and 320 nm

Changes in total body weight (TBW), prostatic weight (PW) and prostatic weight index (PWI)

The PW and PWI were increased significantly in AAH-induced rats. There were no significant changes in PW and PWI after treatment with either, saw palmetto extract (SPE) or SFE except for SFE in a dose of 400 mg which significantly ameliorated the PWI compared to AAH-induced rats (Table 2).

Effect of *S. japonica* fruit extract on cytokine gene expression

The results of the present study showed that induction of AAH in rats significantly increased the gene expression of

Table 2 The effect of *Sophora* fruit extract on total body weight (TBW), prostate weight (PW), and prostate weight index (RPW) in rats with atypical adenomatous hyperplasia (AAH) ($n=7$ rats in each group)

Treatment	TBW (g) start end		PW (g)	PWI (g)
	Start	End		
Normal rats	196.6 ± 6.13	253.6 ± 7.23	0.18 ± 0.01	0.071 ± 0.05
Rats with AAH (negative control)	192.3 ± 7.53	248.4 ± 8.46	0.66 ± 0.05*	0.261 ± 0.19*
Rats with AAH treated with				
Saw Palmetto (100 mg/kg)	190.7 ± 5.44	256.3 ± 7.21	0.61 ± 0.05*	0.238 ± 0.21*
SFE (100 mg/kg)	191.5 ± 4.08	243.5 ± 8.87	0.65 ± 0.04*	0.266 ± 0.21*
SFE (200 mg/kg)	195.3 ± 4.25	258.8 ± 6.74	0.53 ± 0.06*	0.205 ± 0.27*
SFE (400 mg/kg)	196.7 ± 8.76	265.5 ± 8.76	0.34 ± 0.06*	0.128 ± 0.34*,#

*Significantly different from normal rats at $p<0.05$

#Significantly different from AAH rats at $p<0.05$

clusterin, IGF, IL-6, IL-8 and TNF-α; while, the TGF-β1 expression was significantly decreased (Fig. 3a–f). Treatment with SFE induced significant ameliorative effect on the increased levels of IL-8 and TNF-α in a dose-dependent manner (Fig. 3e, f), while in IGF (Fig. 3c), SFE caused significant reduction only in the dose of 400 mg/kg when compared with AAH rat values. In contrast, SFE produced no significant changes in the IL-6 (Fig. 3d) compared to AAH rat values. On the other hand, SFE caused marked and significant increase in clusterin and TGF-β1 even more than normal control rat values (Fig. 3a, b).

Effect of SFE on immunohistochemistry expression of TGFβR-1 and IL-6

Tissue sections from the ventral prostate of normal control rats show no expression of both immunohistochemical markers (TGFβR-1 and IL-6) with positive internal controls (Table 3, Fig. 4a, b). Among the AAH-induced negative control rats, the immunohistochemical expression of TGFβR-1 corresponds to score 3 with strong intensity in the inner epithelial cells of acini. Focal strong expression is also present among the basal epithelial cells. The expression of IL-6 corresponds to score 1 showing weak intensity in the inner epithelial cells only. No expression was observed in basal or stromal cells (Table 3, Fig. 4c, d).

Tissue section of ventral prostate from Saw Palmetto-treated AAH-induced rats shows TGFBR-1 expression corresponding to score 3 exhibiting strong intensity in the inner epithelial cells of acini. IL-6 expression is variable between score 2 with a moderate staining intensity. No expression was observed in basal or stromal cells (Table 3, Fig. 4e, f).

Tissue section of ventral prostate from SFE extract 400 mg/kg treated revealed IL-6 expression corresponding to score 2 with moderate intensity. TGFBR-1 expression was score 3 with strong intensity. No expression was observed in basal or stromal cells. The immunohistochemical profile expressed by the prostatic acini showed no significant dose-related variation (Table 3, Fig. 4g, h).

Histopathological changes

Tissue sections from the ventral prostates of the normal group showed prostatic parenchyma composed of evenly distributed acini embedded in fibromuscular interstitium. The acini are rounded and lined by two layers of epithelium; inner cuboidal and outer flattened. Nuclei are round to oval and are basally placed with finely distributed chromatin. The surrounding interstitium shows mast cells. These findings correspond to a histoscore of 24.3 ± 1.2 (Table 4, Fig. 5a). Tissue sections from the ventral prostates of AAH-induced rats of the control group show an increase in the number of acini (hyperplasia) with uneven distribution. These acini are crowded and show short intraluminal papillary projections. They are lined by two layers of epithelium; outer flattened and inner tall columnar with focal nuclear stratification. Occasional mitosis in the range of 1–2 per 10 high-power fields is noted. The interstitium is scant and edematous. The blood vessels are congested and mixed acute and chronic inflammatory cells and are seen concentrated around them. These findings correspond to a histoscore of 41.1 ± 1.8 (Table 4, Fig. 5b–d). Polymorphonuclear leukocytes with eosinophilic granules are considered as acute inflammatory cells. Chronic inflammatory cells seen are lymphocytes which were distinguished by their darkly stained ink-dot nucleus and a thin rim of bluish cytoplasm.

Tissue sections from the ventral prostrate of AAH-induced rats treated with 100 mg/kg Saw Palmetto show a reduction in the scale of hyperplastic changes which are although persistent when compared to the changes seen in the control group. This is evidenced by the relative decrease in the number of prostatic acini, which are less crowded. There is considerable fibromuscular interstitium with congested blood vessels around the acini. Rare foci of mixed acute and chronic inflammatory cells are also seen. These findings correspond to a histoscore of 32.2 ± 2.1 (Table 4, Fig. 5e).

Tissue sections from the ventral lobe of AAH-induced rats treated with 100 mg/kg SFE extract show two

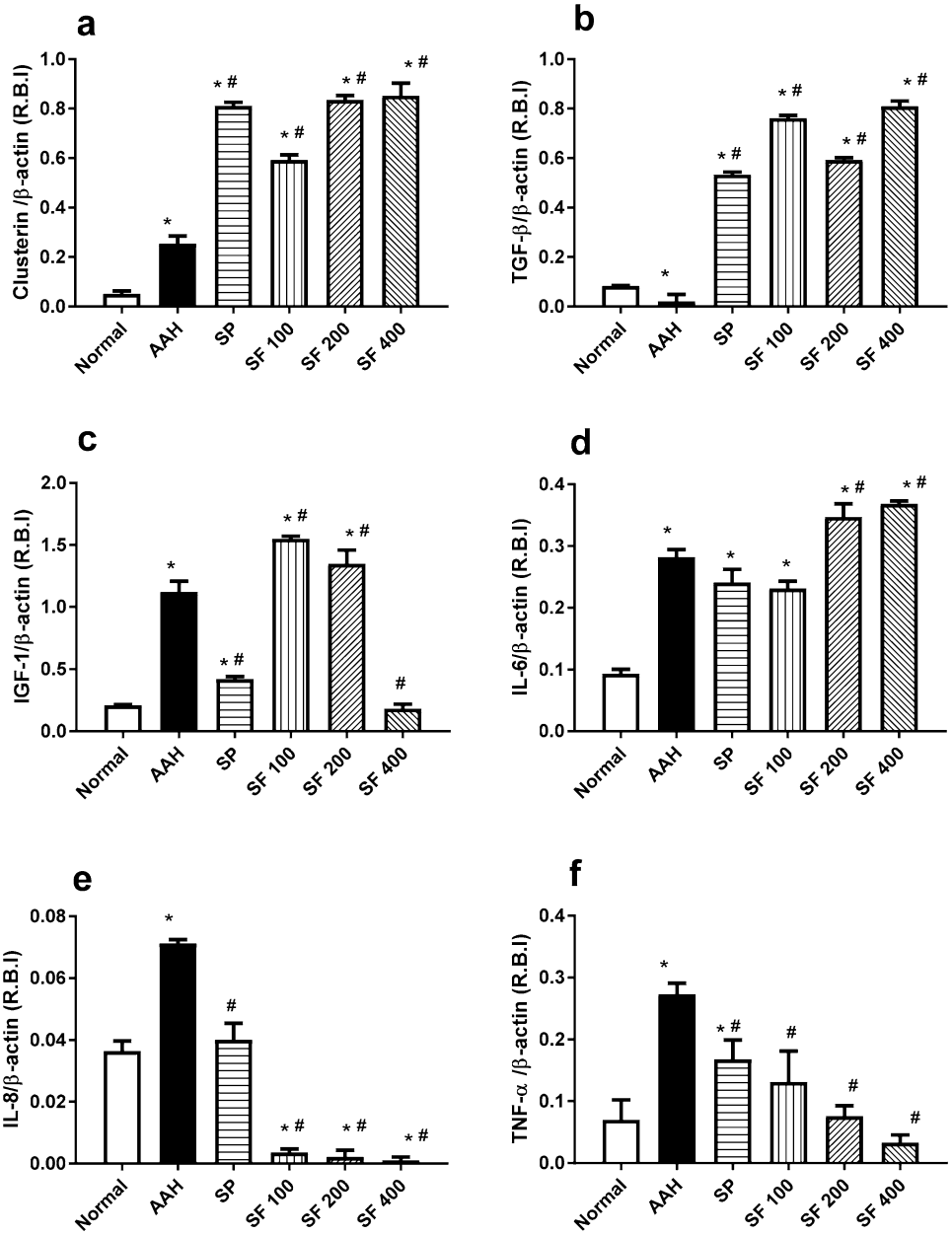

Fig. 3 The effect of different doses of *Sophora* fruit extract on the expression of Clusterin (**a**), TGF-β1 (**b**), IGF-1 (**c**), IL-6 (**d**), IL-8 (**e**) and TNF-α (**f**) target genes in Wistar rats with atypical adenomatous hyperplasia (AAH) compared with normal control rats and those treated with saw palmetto (SP). All values are expressed as mean ± S.E. of the relative band intensity (R.B.I.) using β-actin as a reference. *Significantly different from normal rats at $P < 0.05$. #Significantly different from AAH control rats received CMC at $P < 0.05$

populations of crowded prostatic acini embedded within the scant interstitium. One population of acini appears relatively smaller and shows irregular outlines with short papillary projections into the lumen. These acini are lined by outer flattened and inner tall columnar epithelial cells. Mitotic figures in the inner layer of epithelium are seen in the range of 4–5 per 10 high-power fields among them. The other population of acini is enormously dilated with intraluminal secretions. These acini are lined by low cuboidal epithelium and exhibit no mitosis. The nuclei are oval and basally placed with fine nuclear chromatin in both populations of acini. Both populations of acini show random distribution. No specific zonal pattern is seen. The acini are separated by edematous interstitium which show focal inflammatory cells including mainly neutrophils and mast cells. Dilated congested blood vessels are also seen in the surrounding interstitium. These findings correspond to a histoscore of 40.17 ± 1.93 (Table 4, Fig. 6a–d).

Tissue sections from the ventral lobe of AAH-induced rats treated with 200-mg/kg SFE show the similar scale of changes affecting the acini and interstitium as with those treated with 100-mg/kg SFE. Minor variations are seen in the form of intra-luminal karyorrhectic debris within the acini. The interstitium shows a decrease in the number of both acute and chronic inflammatory cells. The inflammatory cells were marginalized to the periprostatic adipose tissue rather than being located within the parenchyma, which could partially be explained by the nature of biopsy

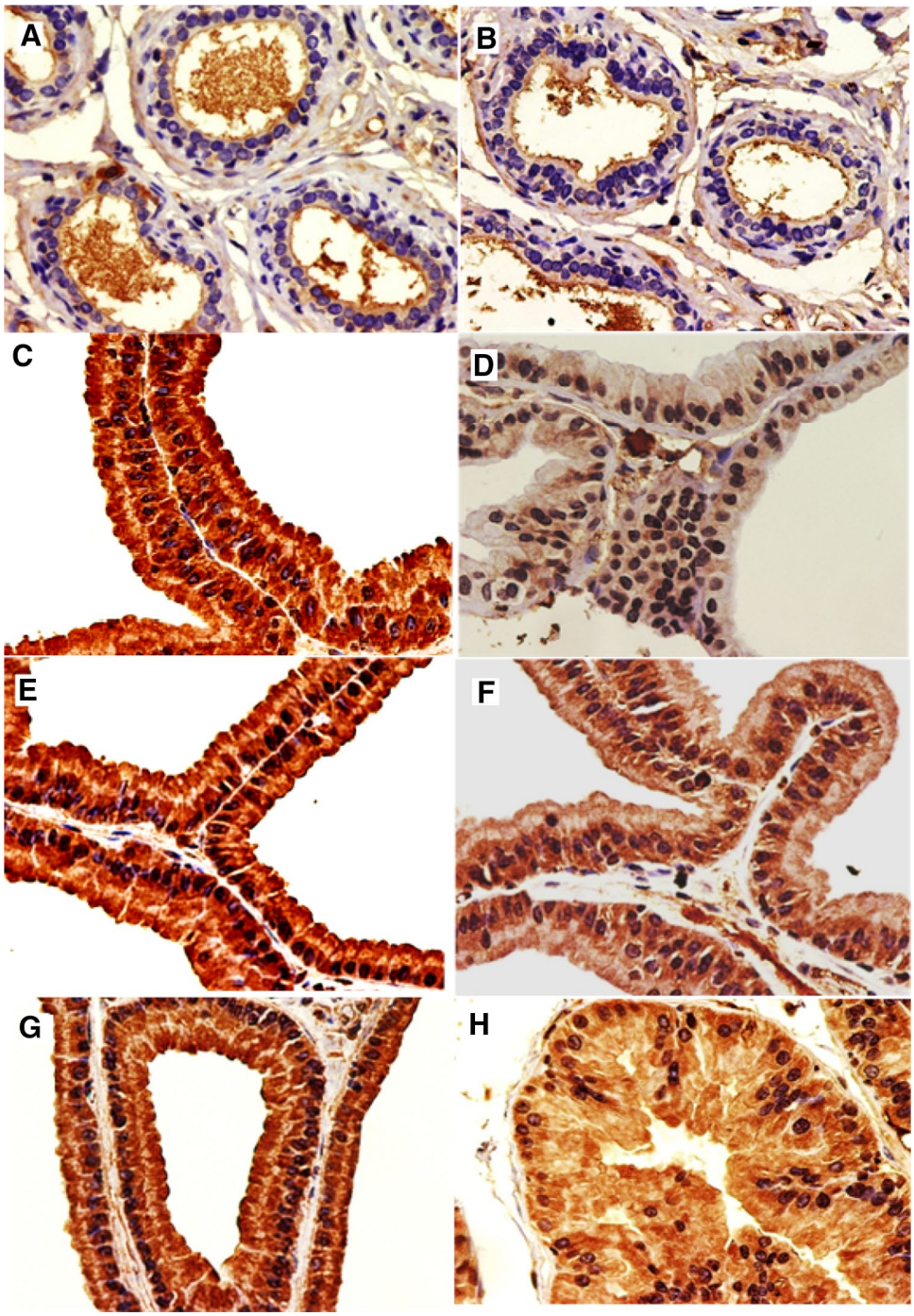

Fig. 4 Tissue section from ventral prostate showing immunohistochemical expression and quantification of TGFBR-1 and IL-6 (X40). **a** Normal rats TGFBR-I expression score 0, **b** normal rats IL-6 expression score 0, **c** AAH control rats TGFBR-1 expression score 3, intensity strong, **d** AAH control rats IL-6 expression score 1, intensity weak. **e** Saw palmetto 100 mg/kg-treated rats TGFBR- 1 score 3, intensity strong. **f** Saw palmetto 100 mg/kg-treated rats IL-6 expression score 2, intensity moderate. **g** Sophora 400 mg/kg-treated rats TGFBR- 1 score 3, intensity strong. **h** Sophora 400 mg/kg-treated rats IL-6 expression score 2, intensity moderate

procedure performed. The findings correspond to a histoscore of 41 ± 2.42 (Table 4, Fig. 6e).

Tissue sections from the ventral lobe of AAH-induced rats treated with 400-mg/kg SFE also show the similar scale of changes affecting the acini and interstitium as with those treated with 100-mg/kg SFE. However, a significant absence of both acute and chronic inflammatory cells within the parenchyma is noted. Mitotic figures seen in the inner layer of epithelium are also reduced and are in the range of 1–2 per 10 high-power fields among them. The findings correspond to a histoscore of 38 ± 1.83 (Table 4, Fig. 6f).

Discussion

In the preset study, testosterone along with citral smearing produced AAH evidenced by increase in both prostatic weight and prostatic weight index of the ventral lobe along

Table 3 Immunohistochemical expression of IL-6 and TGFBR-1 in normal, atypical adenomatous hyperplasia (AAH) control, saw palmetto (SP) and *Sophora* fruit extract-treated AAH-induced rats

Parameters	IHC score in control groups					
	Normal rats	AAH control (CMC 1% treated)	AAH treated with SP 100 mg/kg	AAH treated with SFE 100 mg	AAH treated with SFE 200 mg	AAH treated with SFE 400 mg
IL-6						
Expression	0	1	2	2	2	2
Staining intensity		Weak	Moderate	Moderate	Moderate	Moderate
TGFBR-1						
Expression	0	3	3	3	3	3
Staining intensity		Strong	Strong	Strong	Strong	Strong

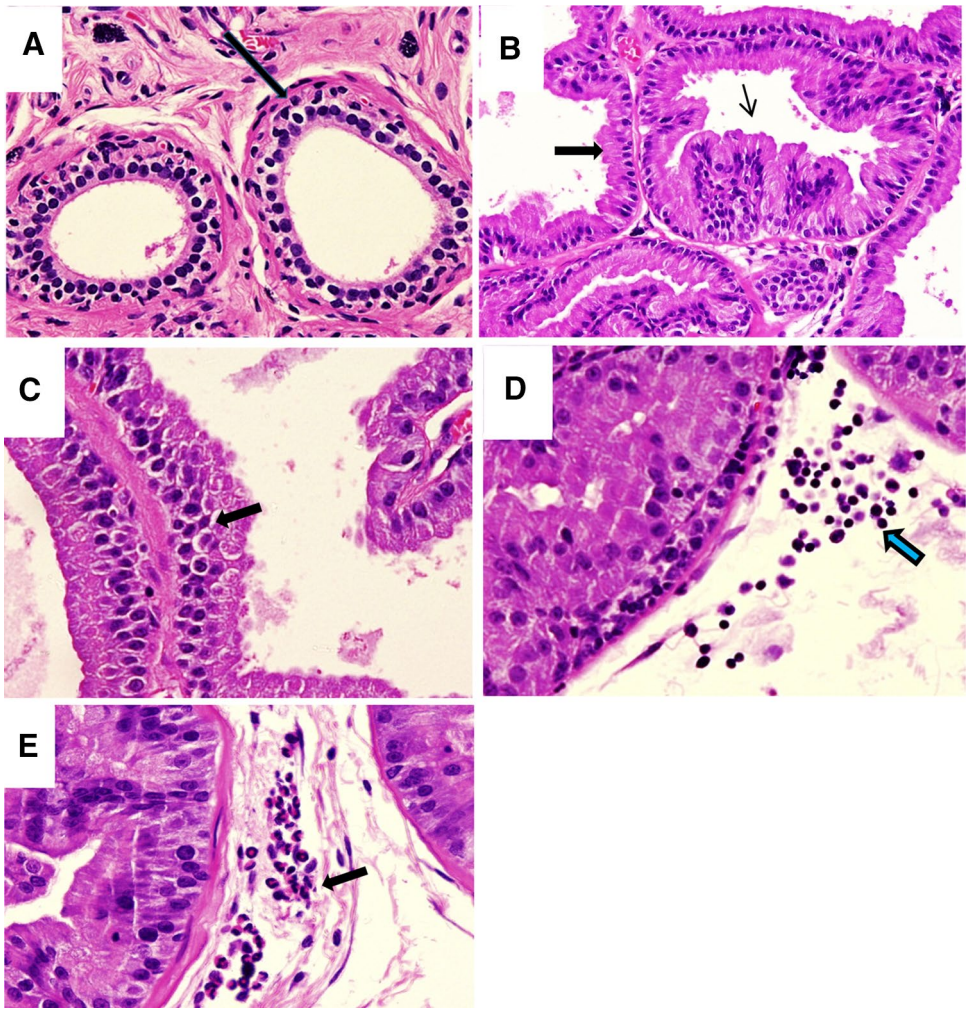

Fig. 5 **a** Tissue section from ventral prostate of normal rats showing even distribution of acini with abundant fibromuscular stroma. Arrow points to acini lined by two layers of epithelium, outer flattened and inner cuboidal. **b** Tissue section from ventral prostate of testosterone and citral-treated castrated rats with atypical adenomatous hyperplasia (AAH) reveal acinar hyperplasia as seen by their crowded appearance with lack of interstitium. Thick arrow points to acini lined by tall columnar cells. Thin arrow points to short intraluminal papillary projections. **c** Tissue section from ventral prostate of testosterone and citral-treated castrated rats with AAH exhibiting nuclear stratification of hyperplastic lining epithelium. **d** Tissue section from ventral prostate of testosterone and citral-treated castrated rats with AAH exhibiting chronic inflammatory cells in the interstitium. Arrow points to a collection of lymphocytes. **e** Tissue section from ventral prostate of saw palmetto-treated rats showing reduced but persistent hyperplastic changes. Arrow points to a focus of polymorphonuclear acute inflammatory cells in the interstitium (×40)

Table 4 Histoscore and inflammatory scores in normal rats, atypical adenomatous hyperplasia (AAH)-induced negative control rats and AAH-induced, saw palmetto-treated (SP) and AAH-induced *Sophora* fruit extract-treated rats

Treatment group	Histoscore	Inflammatory score	Rats in group *N*	Cases of inflammation among tested ratsN=	% Inflammation	% Inhibition of Inflammation
Normal rats	24.3 ± 1.2	0	7	0	–	–
Rats with AAH (negative control)	41.1 ± 1.8*	1	7	7	100	0
Rats with AAH treated with						
SP 100 mg/kg	32.2 ± 2.1*,#	1	6	3	14.28#	85.72#
SF 100 mg/kg	40.17 ± 1.93	1	6	4	25.33#	74.67#
SF 200 mg/kg	41 ± 2.42	1	6	2	22.45#	77.55#
SF 400 mg/kg	38 ± 1.83	0	6	0	18.50#	81.48#

Score 0: no inflammation, score 1: scattered inflammatory cells without nodules, score 2: lymphoid aggregates with no confluence, score 3: large areas of confluence

*Significantly different from normal control rats at $p < 0.05$

#Significantly different from AAH control rats received CMC at $p < 0.05$

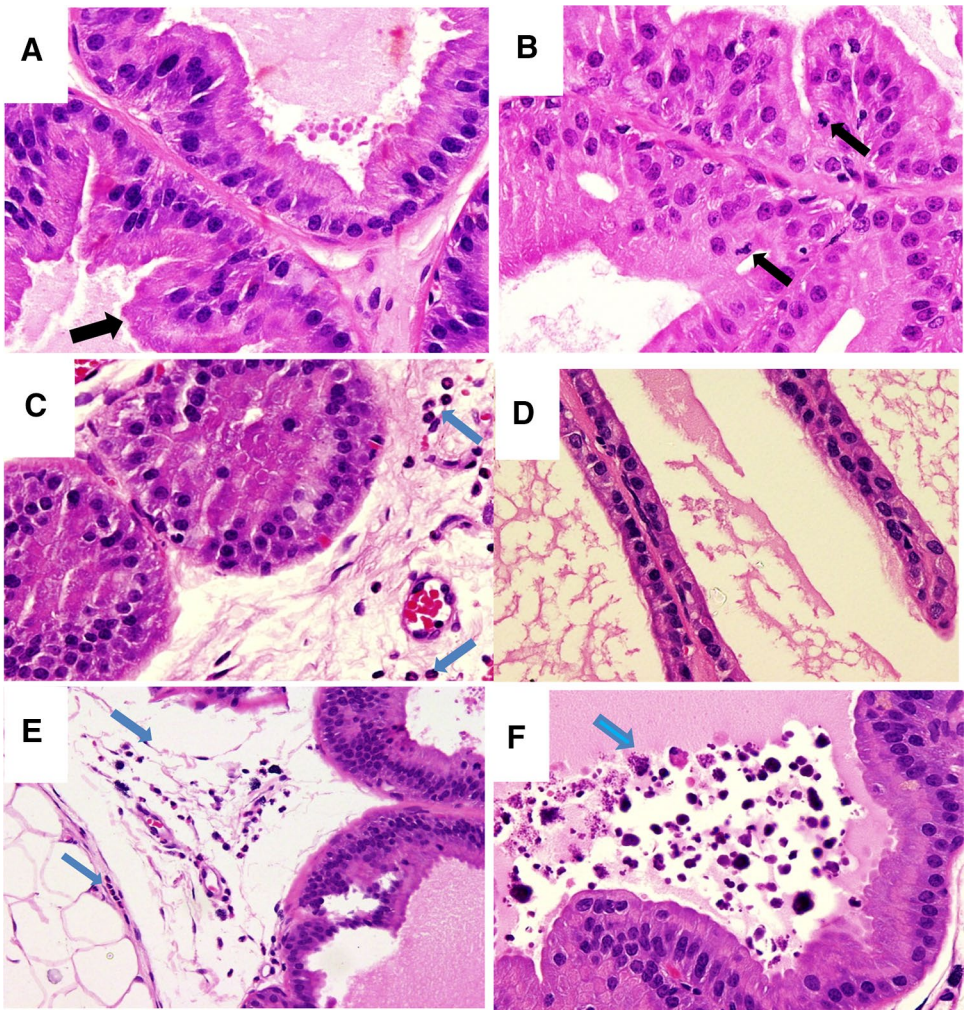

Fig. 6 Tissue section from ventral prostate of rats treated with *Sophora* fruit extract in a dose of 100 mg/kg **a**–**d** showing; **a** Small, crowded acini lined by tall columnar epithelium. Arrow points to short papillary projections into the lumen. **b** Hyperplastic epithelium showing the presence of mitosis at arrows. **c** Interstitial inflammation arrow points to polymorphonuclear acute inflammatory cells. **d** Large dilated acini lined by low cuboidal epithelium with luminal secretions. **e** Tissue section from ventral prostate of rats treated with Sophora extract in a dose of 200 mg/kg showing hyperplastic acinus with intraluminal karyorrhectic debris at the arrow. **f** Tissue section from ventral prostate of rats treated with Sophora extract in a dose of 400 mg/kg showing polymorphonuclear inflammatory cells within the periprostatic adipose tissue at the arrows (×40)

with acinar hyperplasia in histopathological study. It was suggested that AAH induced in adult rats by citral may be attributed to its estrogenic-like effect through its binding non-specifically to estrogen receptors located on prostate epithelial cells (Engelstein et al. 1996). In addition, the AAH-induced rats showed increased gene expression of IGF-1 and decreased TGF-β1. There are two major classes of growth factors, growth stimulatory factors as IGFs which promote the cell proliferation (Biernacka et al. 2012) and growth inhibitory factors as TGF-β1 that repress the expression of E-cadherin, which is a tumor suppressor (Xu et al. 2017). Moreover, previous studies showed that inflammation play an important role in prostatic hyperplasia (Kramer and Marberger 2006) which is in accordance with the results of the present study that revealed over-expression of the pro-inflammatory cytokines including IL-6, IL-8 and TNF-α in AAH-induced rats.

The results of the present study showed that administration of SFE ameliorated the proinflammatory cytokine expression, the inflammatory score, and histopathological changes in AAH-induced rats in a dose-dependent manner. These findings are in agreement with the results of Kim and colleagues (2013), which revealed the anti-inflammatory effect of sophoricoside, an isoflavone glycoside isolated from SFE and revealed a selective inhibitory effect on cyclooxygenase (COX-2) activity. Moreover, (Dong et al. 2013) showed that oxymatrine, a potent monosomic alkaloid extracted from *S. japonica,* possesses anti-inflammatory activity through inhibition of the productions of PGE2, TNF-α, IL-1β and IL-6 which is evident in the present study. In addition, gallic acid, a phenolic compound isolated previously from SF, which was found to have anti-inflammatory effect through inhibition of TNF-α, IL-1β (Owumi et al. 2020). Previous studies found that gallic acid has also an anticancer effect through induction of apoptosis (Tang and Cheung 2019; Kang et al. 2020). This is in accordance with the histopathological changes of the current study which revealed that SFE in a dose of 400 mg caused a reduction of the mitotic changes seen in the inner layer of epithelium in AAH-induced rats. Results of the present study showed that SFE increased the expression of TGF-βI, while decreased the expression of IGF-1 especially in a dose of 400 mg/kg in rat ventral lobe prostate. Overexpression of TGF-β1 showed the increased rate of apoptosis of acini on the ventral prostate. On the other hand, quercetin derivatives present in the SFE (Li et al. 2002) suppressed the proliferation of human prostate cancer cells via multiple signaling pathway and promote cancer prostate through inhibition of epithelial–mesenchymal transition process (Lu et al. 2020).

Despite that, treatment with SFE failed to ameliorate the elevated level of clusterin. Instead, it even aggravated its increased level. Clusterin is a conserved glycoprotein that plays a key role in cellular stress response and survival and evidence has demonstrated that clusterin is overexpressed in tumor metastasis. Clusterin has been shown to have the role in anti-apoptotic capacities, treatment of the resistance and induction of epithelial–mesenchymal transition, all associated with cancer metastasis (Peng et al. 2019). The conflicting results regarding clusterin may be explained by that there are two isoforms (1 and 2) with antagonistic actions regarding apoptosis (Koltai 2014).

Conclusion

The findings of the present study suggest that methanolic extract of SFE has ameliorating effect on the prostatic hypertrophy and inflammation. This effect may be attributed to the ability of SFE to decrease the production of pro-inflammatory cytokines, TNF-α, IL-1β and IGF-1 as well as increase in TGF-β1.

Acknowledgements This work was supported by Sheikh Ahmed H. Fetaihi, Chair for Research on Prostatic Diseases, King Abdulaziz University, Jeddah, Saudi Arabia. We would like also to thank Mr. Islam Farouk, Department of Pharmacology and Toxicology, Faculty of Pharmacy, King Abdulaziz University, Jeddah, Saudi Arabia for his great effort and help in the experimental study.

Compliance with ethical standards

Conflict of interest The authors declare that they have no competing interests.

References

Abdallah HM, Al-Abd AM, Asaad GF, Abdel-Naim AB, El-Halawany AM (2014) Isolation of antiosteoporotic compounds from seeds of *Sophora japonica*. PLoS ONE 9:e98559

Abdel-Sattar EA, Mouneir SM, Asaad GF, Abdallah HM (2014) Protective effect of *Calligonum comosum* on haloperidol-induced oxidative stress in rat. Toxicol Ind Health 30:147–153

Biernacka K, Perks C, Holly J (2012) Role of the IGF axis in prostate cancer progression. Minerva Endocrinol 37:173–185

Bostwick DG et al (1993) Atypical adenomatous hyperplasia of the prostate: morphologic criteria for its distinction from well-differentiated carcinoma. Hum Pathol 24:819–832

Chinese-Pharmacopoeia-Commission (2010) Pharmacopoeia of the People's Republic of China 2010. China Medical Science and Technology Press, Beijing, pp 61–62

De Nunzio C et al (2011) The controversial relationship between benign prostatic hyperplasia and prostate cancer: the role of inflammation. Eur Urol 60:106–117

Dong X-Q et al (2013) Anti-inflammatory effects of oxymatrine through inhibition of nuclear factor–kappa b and mitogen-activated protein kinase activation in lipopolysaccharide-induced BV2 microglia cells. Iran J Pharm Res 12:165

Enciu M, Aşchie M, Boşoteanu M, Chisoi A (2012) Atypical adenomatous hyperplasia of the prostate mimicking adenocarcinoma lesion: case report and literature review. Rom J Morphol Embryol 53:1093–1096

Engelstein D, Shmueli J, Bruhis S, Servadio C, Abramovici A (1996) Citral and testosterone interactions in inducing benign and atypical prostatic hyperplasia in rats. Comp Biochem Physiol Part C: Pharmacol Toxicol Endocrinol 115:169–177

Gleason PE et al (1993) Platelet derived growth factor (PDGF), androgens and inflammation: possible etiologic factors in the development of prostatic hyperplasia. J Urol 149:1586–1592

Golomb E, Kruglikova A, Dvir D, Parnes N, Abramovici A (1998) Induction of atypical prostatic hyperplasia in rats by sympathomimetic stimulation. Prostate 34:214–221

Gounder S et al (2008) Prostate cancer immunohistochemical (IHC) stains and survival in stage D3 patients (pts). J Clin Oncol 26:22187

Ho JW, Hon PL, Chim WO (2009) Effects of oxymatrine from Ku Shen on cancer cells. Anti-Cancer Agents Med Chem (Former Curr Med Chem-Anti-Cancer Agents) 9:823–826

Hobisch A et al (2000) Immunohistochemical localization of interleukin-6 and its receptor in benign, premalignant and malignant prostate tissue. J Pathol 191:239–244

Humphrey PA (2012) Atypical adenomatous hyperplasia (adenosis) of the prostate. J Urol 188:2371–2372

Jin JH, Kim JS, Kang SS, Son KH, Chang HW, Kim HP (2010) Anti-inflammatory and anti-arthritic activity of total flavonoids of the roots of *Sophora flavescens*. J Ethnopharmacol 127:589–595

Kang DY et al (2020) The inhibitory mechanisms of tumor PD-L1 expression by natural bioactive gallic acid in non-small-cell lung cancer (NCLC) cells. Cancers 12:727

Kessler OJ, Keisari Y, Servadio C, Abramovici A (1998) Role of chronic inflammation in the promotion of prostatic hyperplasia in rats. J Urol 159:1049–1053

Kim BH, Chung EY, Min B-K, Lee SH, Kim M-K, Min KR, Kim Y (2003) Anti-inflammatory action of legume isoflavonoid sophoricoside through inhibition on cyclooxygenase-2 activity. Planta Med 69:474–476

Koltai T (2014) Clusterin: a key player in cancer chemoresistance and its inhibition. OncoTargets Ther 7:447

Kramer G, Marberger M (2006) Could inflammation be a key component in the progression of benign prostatic hyperplasia? Curr Opin Urol 16:25–29

Lamaison J, Petitjean-Freytet C, Carnat A (1990) Rosmarinic acid, total hydroxycinnamic derivatives and antioxidant activity of Apiaceae, Borraginaceae and Lamiceae medicinals. Annal Pharm Francaises 48:103–108

Li X, Zhang Y, Yuan Z (2002) Separation and determination of rutin and quercetin in the flowers of *Sophora japonica* L. by capillary electrophoresis with electrochemical detection. Chromatographia 55:243–246

Lillie R, Fullmer H (1965) Histopathologic technic and practical histochemistry, 3rd edn. McGraw-Hill Book Company, New York

Lu X, Chen D, Yang F, Xing N (2020) Quercetin inhibits epithelial-to-mesenchymal transition (EMT) process and promotes apoptosis in prostate cancer via downregulating lncRNA MALAT1. Cancer Manag Res 12:1741

Montironi R, Mazzucchelli R, Lopez-Beltran A, Cheng L, Scarpelli M (2007) Mechanisms of disease: high-grade prostatic intraepithelial neoplasia and other proposed preneoplastic lesions in the prostate. Nat Clin Pract Urol 4:321–332

Owumi SE, Nwozo SO, Effiong ME, Najophe ES (2020) Gallic acid and omega-3 fatty acids decrease inflammatory and oxidative stress in manganese-treated rats. Exp Biol Med. https://doi.org/10.1177/1535370220917643

Peng M, Deng J, Zhou S, Tao T, Su Q, Yang X, Yang X (2019) The role of clusterin in cancer metastasis. Cancer Manag Res 11:2405

Pu L-P, Chen H-P, Cao M-A, Zhang X-L, Gao Q-X, Yuan C-S, Wang C-M (2013) The antiangiogenic activity of Kushecarpin D, a novel flavonoid isolated from *Sophora flavescens* Ait. Life Sci 93:791–797

Rigas B, Sun Y (2008) Induction of oxidative stress as a mechanism of action of chemopreventive agents against cancer. Br J Cancer 98:1157–1160

Sandford NL, Searle J, Kerr J (1984) Successive waves of apoptosis in the rat prostate after repeated withdrawal of testosterone stimulation. Pathology 16:406–410

Sciarra A, Mariotti G, Salciccia S, Gomez AA, Monti S, Toscano V, Di Silverio F (2008) Prostate growth and inflammation. J Steroid Biochem Mol Biol 108:254–260

Scolnik MD, Servadio C, Abramovici A (1994) Comparative study of experimentally induced benign and atypical hyperplasia in the ventral prostate of different sat strains. J Androl 15:287–297

Singleton VL, Rossi JA (1965) Colorimetry of total phenolics with phosphomolybdic-phosphotungstic acid reagents. Am J Enol Viticult 16:144–158

Sun M, Cao H, Sun L, Dong S, Bian Y, Han J, Zhang L, Ren S, Hu Y, Liu C, Xu L (2012) Antitumor activities of kushen: literature review. Evid Based Complement Altern Med 2012:373219

Tang HM, Cheung PCK (2019) Gallic acid triggers iron-dependent cell death with apoptotic, ferroptotic, and necroptotic features. Toxins 11:492

Xu H et al (2017) DNMT1 regulates IL-6-and TGF-β1-induced epithelial mesenchymal transition in prostate epithelial cells. Eur J Histochem. 61:2775

Zhang B et al (2011) Antiinflammatory effects of matrine in LPS-induced acute lung injury in mice. Eur J Pharm Sci 44:573–579

Zhang W et al (2015) Simultaneous extraction and purification of alkaloids from *Sophora flavescens* Ait. by microwave-assisted aqueous two-phase extraction with ethanol/ammonia sulfate system. Sep Purif Technol 141:113–123

Zhou H, Lutterodt H, Cheng Z, Yu L (2009) Anti-inflammatory and antiproliferative activities of trifolirhizin, a flavonoid from *Sophora flavescens* roots. J Agric Food Chem 57:4580–4585